

Air Toxics Hot Spots Program

Perchloroethylene Inhalation Cancer Unit Risk Factor

Technical Support Document for Cancer
Potency Factors

Appendix B

Public Review Draft

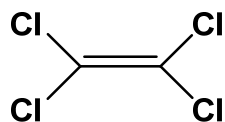
February 2016



Air, Community, and Environmental Research Branch
Office of Environmental Health Hazard Assessment
California Environmental Protection Agency

Page left intentionally blank

PERCHLOROETHYLENE



CAS Number: 127-18-4

1. INTRODUCTION

The Office of Environmental Health Hazard Assessment (OEHHA) develops potency values for carcinogenic substances that are candidate Toxic Air Contaminants (TACs) (Health and Safety Code Section 39660) or are listed under the Air Toxics Hot Spots Act (Health and Safety Code Section 44321). These values are used in the Air Resources Board's (ARB's) air toxics control programs and also by other State regulatory bodies, to estimate cancer risk in humans .

Perchloroethylene (PCE), also commonly referred to as tetrachloroethylene, was officially placed on the TAC list by the ARB in 1991. In support of that decision, the California Department of Health Services evaluated the toxicology of PCE and determined that it was a potential carcinogen in humans, besides displaying other forms of toxicity (CDHS, 1991). Shortly thereafter, OEHHA derived inhalation potency values for PCE using dose-response data from a National Toxicology Program (NTP) study of the chemical's carcinogenic effects in rodents (OEHHA, 1992; NTP, 1986). OEHHA's potency values were based upon the induction of liver tumors in male mice and incorporated a simple pharmacokinetic model to estimate internal metabolized doses.

The present document updates the dose-response analysis for inhalation exposure to PCE to derive a cancer unit risk factor (expressed as $(\mu\text{g}/\text{m}^3)^{-1}$) and a corresponding cancer slope factor (expressed in $(\text{mg}/\text{kg}\cdot\text{d})^{-1}$) using OEHHA's current Air Toxics Hot Spots program risk assessment guidelines (OEHHA, 2009), and research made available since our last PCE review in 1992. In particular, OEHHA has identified an additional well-conducted, lifetime rodent inhalation study (JISA, 1993); also, a refined physiologically-based pharmacokinetic (PBPK) model for PCE has been published (Chiu and Ginsberg, 2011). Both of these studies were used in the update. Where appropriate, the current analysis draws upon material from previous OEHHA evaluations, as well as recent toxicological assessments published by the US Environmental Protection Agency (US EPA, 2012a) and the International Agency for Research on Cancer (IARC, 2014).

2. SUMMARY OF DERIVED VALUES

OEHHA's revised potency values for PCE are based on the elevated incidence of several tumor types observed in male mice and rats in relation to PCE-metabolized doses calculated with a simplified adaptation of the Chiu and Ginsberg (2011) model. For dose-response calculations, OEHHA used US EPA's Benchmark Dose Software (BMDS) (US EPA, 2015) and its implementation of the multi-stage cancer model. BMDS was also

used to evaluate the multi-site tumor risks. After considering several issues related to data quality and analytical uncertainty, the geometric mean of 4 dose-response values was chosen as the best estimate of carcinogenic potency. The potency values for PCE, in terms of external exposure, are:

Unit Risk Factor ($\mu\text{g}/\text{m}^3$) ⁻¹	6.1E-06
Slope Factor ($\text{mg}/\text{kg}\cdot\text{day}$) ⁻¹	2.1E-02

3. MAJOR SOURCES AND USES

PCE is a dense volatile liquid with an ether-like odor. It is used mainly as a chemical intermediate, solvent, and cleaning agent. The total US demand for PCE in 2004 was 355 million pounds (Dow, 2008). In the US, 60 percent of PCE use was for chemical production (e.g., to make hydrofluorocarbon alternatives to chlorofluorocarbons), 18 percent was used in surface preparation and cleaning, 18 percent in dry-cleaning and textile processing, and 4 percent for miscellaneous other uses (*ibid.*). Total air emissions of PCE in California for 2010 were estimated by ARB to be 3832 tons per year (ARB, 2012).

4. SELECTED PHYSICAL AND CHEMICAL PROPERTIES OF PCE

Molecular weight	165.83
Boiling point	121 °C
Melting point	-19 °C
Vapor pressure	18.47 mm Hg @ 25 °C
Air concentration conversion	1 ppm = 6.78 mg/m ³ @ 25 °C

(HSDB, 2010)

5. NATIONAL AND INTERNATIONAL HAZARD EVALUATIONS

According to the National Toxicology Program (NTP) 13th Report on Carcinogens, PCE is "reasonably anticipated to be a human carcinogen based on sufficient evidence of carcinogenicity from studies in experimental animals" (NTP, 2014). The NTP report noted that PCE exposure produced tumors in multiple tissue types of both sexes of mice and rats, by ingestion and/or inhalation. The tumor types cited by NTP were: mononuclear-cell leukemia in rats, tubular-cell kidney tumors in male rats and liver tumors in mice.

IARC found that PCE is "probably carcinogenic to humans," citing limited epidemiological findings (primarily increased bladder cancer in dry cleaning workers) and sufficient evidence in experimental animals (IARC, 2014). For rodents, in addition to the tumor types noted by NTP, IARC notes increased incidence of: hemangioma and hemangiosarcoma of the liver in mice, spleen and Harderian gland tumors in male mice, brain and testicular tumors in male rats, and skin tumors in mice dermally exposed to PCE metabolite, tetrachloroethylene oxide.

US EPA states that PCE is “likely to be carcinogenic in humans by all routes of exposure,” based upon suggestive epidemiologic data (bladder cancer, non-Hodgkin’s lymphoma, and multiple myeloma) and conclusive evidence from carcinogenicity studies in rodents (referring to the same set of tumors as above) (U.S. EPA, 2012b).

PCE has been listed on California’s Proposition 65 list since 1988 as a chemical “known to the state to cause cancer.” California’s Public Health Goal for drinking water is based on carcinogenicity concerns (OEHHA, 2001).

6. TOXICOKINETICS

PCE is readily absorbed through the lungs and gastrointestinal tract, and can also be absorbed to a lesser extent through the skin. The blood-air partition coefficients of PCE in humans and rodents are in the range of about 15 to 20 (Chiu and Ginsberg, 2011). These values indicate the ratio by which the PCE concentration in blood will be greater than its concentration in air at equilibrium. Humans breathing air containing 100 ppm PCE over 8 hours absorbed approximately 70 percent of inhaled PCE after the first hour, and 50 percent of the PCE intake at the end of the exposure period (Fernandez, *et al.*, 1976). Once in the body, PCE disperses into all tissues, concentrating preferentially in fatty tissues. For example, in rats inhaling 500 ppm PCE for 2 hours, the area under the concentration curve (AUC) after 72 hours, in milligram-minutes per milliliter of tissue, was: 1493 (fat), 33 (brain), 31 (liver), 26 (kidney), and 8.4 (blood) (Dallas, *et al.*, 1994).

PCE has a relatively low rate of metabolism in rodents and humans and is primarily eliminated unchanged via exhalation. In rats exposed to 150 ppm PCE in drinking water for 12 hours and monitored for an additional 72 hours, approximately 88% of the body burden was eliminated unmetabolized by exhalation (Frantz and Watanabe, 1983). Ohtsuki, *et al.* (1983) monitored occupationally exposed dry-cleaning workers and estimated that at the end of an 8-hour exposure to 50 ppm, about 38% of absorbed PCE was exhaled unchanged and 2% metabolized and excreted in urine.

PCE Metabolites

The metabolism of perchloroethylene has been studied mostly in mice, rats, and humans. Detailed reviews of this literature have been published (Lash and Parker, 2001; Anders *et al.*, 1988; Dekant, 1986). Briefly, rodent studies have identified the following urinary metabolites:

- trichloroacetic acid (TCA)
- N-trichloroacetyl aminoethanol
- oxalic acid
- N-oxalylaminoethanol
- dichloroacetic acid (DCA)
- S-(1,2,2-trichlorovinyl)glutathione (TCVG)
- N-acetyl-S-(1,2,2-trichlorovinyl)cysteine (N-AcTCVC)

Trichloroacetic acid and N-AcTCVC have also been observed in the urine of exposed humans. The aminoethanol derivatives, N-trichloroacetyl aminoethanol and oxalyl aminoethanol, are thought to arise from the reaction of the intermediate acyl chlorides with phosphatidyl ethanolamine present in biological membranes (Dekant, *et al.*, 1986). Carbon dioxide has also been found as an exhaled metabolite. Trichloroethanol has been detected in urine samples in some studies, but not in others, and it is unclear whether it was produced from co-exposure to trichloroethylene (in occupational exposures), or in other cases, if it was an artifact of the analytical methods employed (Lash and Parker, 2001). More recent work (e.g., Yoshioka, *et al.*, 2002) has not detected trichloroethanol and supports the conclusion that it is not a significant PCE metabolite (U.S. EPA, 2012a).

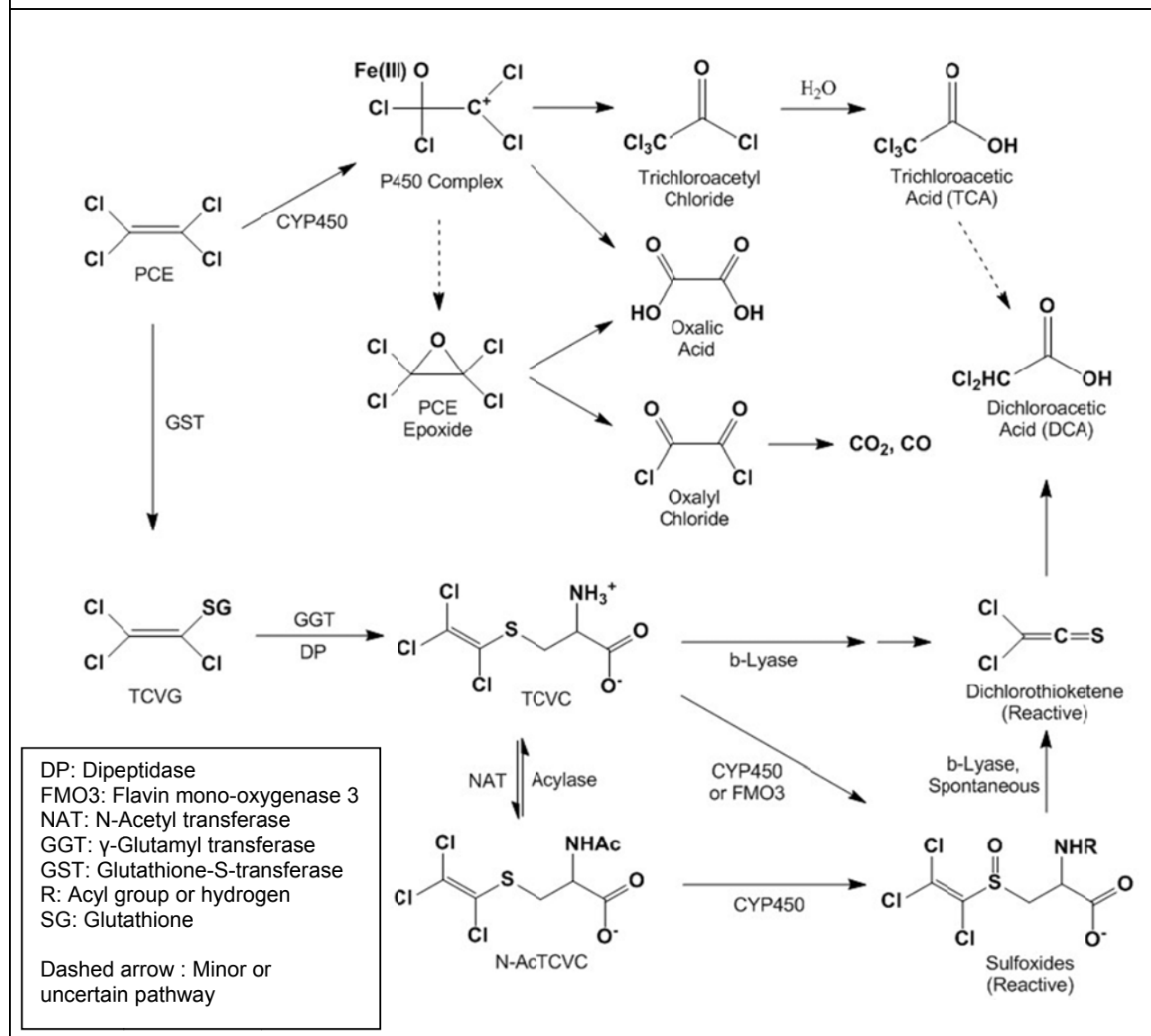
A simplified metabolic scheme for PCE is presented in Figure 1. Two main pathways of metabolism have been identified. The first, referred to here as the "oxidative pathway," involves oxidation of PCE by Cytochrome P450 (CYP450) enzymes. CYP2E1 is thought to be the primary isoform involved, with additional participation of isoforms 2B1/2, and 3A4. The main metabolic product of the oxidative pathway is trichloroacetic acid (TCA), formed by hydrolysis of intermediate trichloroacetyl chloride, the latter of which appears to be formed by molecular rearrangement of the substrate-CYP450 complex (Guyton, *et al.*, 2014).

A secondary product is the reactive tetrachloroethylene oxide (PCE epoxide), which decomposes to oxalyl chloride and then to carbon monoxide and carbon dioxide (Yoshioka, *et al.*, 2002). Oxalic acid may also form from decomposition of PCE epoxide or directly from the substrate-enzyme complex. (Guyton *et al.*, 2014).

The second metabolic pathway for PCE (the "GST pathway") is initiated by glutathione-S-transferase (GST)-catalyzed conjugation with glutathione, forming S-(trichlorovinyl)glutathione (TCVG). This conjugate can undergo additional enzymatic transformations to reactive and potentially genotoxic intermediates. First, the tripeptide glutathione moiety of TCVG is degraded via hydrolytic cleavage of its glycine and glutamine units, producing S-(trichlorovinyl)cysteine (TCVC). TCVC may be subsequently transformed as follows:

- The free amino group of TCVC may be acylated by N-acetyl transferase, forming N-acetyl-S-(trichlorovinyl)cysteine (N-AcTCVC) which passes into urine; this process may also be reversed by acylases, regenerating TCVC.
- The sulfur atom of TCVC and N-AcTCVC may be oxidized by CYP450 or flavin-containing mono-oxygenase 3 (FMO3); this process forms reactive α,β -unsaturated sulfoxides that can bond with nucleophilic biological molecules or spontaneously decompose to dichlorothioketene, itself a reactive metabolite.
- The carbon-sulfur bond of TCVC may be cleaved by β -lyase, releasing an unstable trichlorovinyl thiol that spontaneously decomposes to dichlorothioketene.

Figure 1: Simplified Metabolic Scheme for PCE^(a)



(a) From Guyton *et al.* (2014), U.S. EPA (2012a), and Lash and Parker (2001).

Dichloroacetic acid, believed to arise mainly by hydrolysis of dichlorothioketene, was found in rat but not human urine. Evidence for this mechanism comes from the detection of a covalent protein adduct, N-(dichloroacetyl)-L-lysine in rat kidney cells (Birner *et al.*, 1994)

Multi-Organ Metabolism

The toxicokinetic behavior of PCE is somewhat complicated due to the variety of potentially genotoxic metabolites that can be produced, and because significant PCE metabolism occurs in both the liver and kidney (and possibly other organs as well). The liver is considered the main site of metabolism for the oxidative pathway. This pathway is relatively simple: initial oxidation by CYP450 produces several reactive intermediates

that can rearrange, hydrolyze, undergo conjugation, and otherwise decompose to more stable and soluble metabolites that can then be eliminated in the urine or by exhalation. Other tissues with appropriate CYP450 activity, e.g., lung, kidney, brain, and lymphocytes,¹ may also independently oxidize PCE, though to a smaller extent.

The GST pathway, on the other hand, is more complex. It involves a series of enzymatic transformations with cycling of metabolic intermediates mainly between the liver and kidney, and including some entero-hepatic processing. In this pathway, the initial glutathione conjugation step occurs primarily in the liver, forming TCVG which is then transported to the blood and bile. The kidney epithelium actively absorbs the circulating glutathione conjugate for further processing and excretion. As noted above, this involves cleavage of TCVG by gamma glutamyl transferase (GGT) and dipeptidase (DP) to form TCVC. The amino group of TCVC can then be acylated to form mercapturate N-AcTCVC in the kidney, or TCVC may recirculate back to the liver for acylation (Lash and Parker, 2001).

In some species, such as rabbit and guinea pig, significant intrahepatic processing of glutathione conjugates may occur, with formation of TCVC from TCVG by the bile-duct epithelium, followed by reabsorption into hepatocytes and subsequent acylation. Additionally, TCVG excreted via the bile can be converted to TCVC in the intestinal lumen and undergo entero-hepatic cycling (Hinchman and Ballatori, 1994; Irving and Elfarra, 2013).

The kidney is viewed as the main site for formation of genotoxic metabolites by β -lyase cleavage of TCVC since β -lyase activity is relatively high in this organ. Smaller amounts of β -lyase have been found in other organs, such as the liver, brain, and spleen (Rooseboom, *et al.*, 2002), raising the possibility that reactive dichloroacetene (see Figure 1) may be generated and produce genetic damage in other tissues independent of its production in the kidney. Although the liver contains a form of β -lyase, enzymatic cleavage of TCVC does not appear to be significant in this organ. For example, in rats treated with the PCE-conjugate analogues, dichlorovinyl glutathione (DCVG) and dichlorovinyl cysteine (DCVC), significant pathology was observed in the kidney, but no tissue damage was seen in the liver (Lash and Parker, 2001).

Oxidation of TCVC and N-AcTCVC to the reactive α,β -unsaturated sulfoxides can occur in the liver and kidney, as well as other organs that contain Flavin mono-oxygenase 3 (FMO3) or CYP450 3A activity. As noted above, the sulfoxides are reactive Michael acceptors and can bond with nucleophilic sites on biological molecules. Discussing the metabolism of trichloroethylene (TCE), Irving and Elfarra (2012) noted that the α,β -unsaturated sulfoxides formed in the GST pathway may be further conjugated with glutathione, but that this process is reversible. This creates a mechanism by which the reactive sulfoxides can circulate in a stabilized form through the blood to other organs where they may be reactivated. The mechanism is likely operative for PCE as well.

¹ Lymphocyte microsomes from male Wistar rats have been found to contain CYP450 2B, 2E, and 3A activity at 20, 4, and 2.4 percent of liver microsomal activity. Lymphocyte CYP450 content can also be chemically induced, resulting in 2 to 4-fold increases in activity (Hannon-Fletcher and Barnett, 2008).

Pharmacokinetic Model

Numerous physiologically based pharmacokinetic (PBPK) models have been proposed for PCE over the course of several decades. Reddy (2005), Clewell (2005), and US EPA (2012a) have reviewed this body of research. Although the models are reasonably consistent in estimating PCE blood concentrations, they differ widely in their predictions of metabolized PCE at lower exposure concentrations. For example, at an inhaled concentration of 1 ppb, some models predict about 1 or 2 percent metabolism, while others predict metabolism in the range of 20 to 35 percent, and perhaps as high as 60 percent (Chiu and Ginsberg, 2011). Since PCE's carcinogenic potency is likely to depend upon the formation of genotoxic metabolic products, the wide range of estimated PCE metabolism among models has been a recognized problem for assessing the cancer risk from low-level PCE exposure.

The most recent and comprehensive PBPK model for PCE is that of Chiu and Ginsberg (2011). It was developed following the recommendations of the National Research Council (NRC, 2010) that the available models for PCE be integrated into a single harmonized model incorporating various improvements. The most important improvements of the Chiu and Ginsberg model, as discussed by the U.S. EPA (2012a), are:

- It uses Bayesian Markov Chain Monte Carlo (MCMC) methodology to determine the most likely values (posterior modes) for key metabolic constants.
- The model is calibrated using all of the available toxicokinetic data for PCE in mice, rats, and humans.
- It is the first model to include a separate glutathione conjugation pathway.
- It incorporates recent information on TCA toxicokinetics from trichloroethylene modeling studies.

Table 2 shows a summary of model predictions for several types of dose-metric, as reported by Chiu and Ginsberg (2011). The prediction range of the dose-metric estimates was narrow for both PCE AUC (<20%) and oxidation (<1.5-fold). In contrast, the dose metrics for the GST conjugation pathway in mice and humans displayed significantly higher variability. In the human model, the MCMC analysis produced an apparently bimodal distribution with an approximately 3000-fold difference between the two posterior modes. Chiu and Ginsberg (2011) were not able to determine how much of the spread was due to model uncertainty or population variation, but noted that the distribution could represent actual variability given the large differences in GST activities displayed by humans for some enzyme genotypes. On the other hand, a high level of variability was not observed in metabolic studies of trichloroethylene (TCE): Lash *et al.* (1999) looked at rates of TCE glutathione conjugation in 40 ethnically and age-diverse, male and female human liver samples and found less than a 10-fold variation.

Table 2: PCE Internal Dose Metrics from the Chiu and Ginsberg (2011) PBPK Model^(a)
Inhalation Dose (posterior mode estimates)

Dose metric	Exposure Concentration (ppm)				Prediction Range
	0.01	1	10	100	
<i>PCE AUC Blood</i>	<i>(mg-l)/(hr-d) per ppm</i>				
Mouse	2.1	2.1	2.4	2.6	< 10%
Rat	2.3	2.3	2.3	2.3	< 10%
Human	2.0	2.0	2.0	2.0	< 20%
<i>PCE Oxidation</i>	<i>Percent of intake that is oxidized</i>				
Mouse	18.8	17.4	11.8	7.3	< 40%
Rat	4.2	4.2	4.1	3.3	< 20%
Human	0.98	0.98	0.98	0.98	< 1.5-fold
<i>PCE Conjugation</i>	<i>Percent of intake that is conjugated</i>				
Mouse	0.015	0.016	0.021	0.025	~ 60-fold
Rat	0.31	0.31	0.31	0.32	< 30%
Human	9.4	9.4	9.4	9.4	~ 3000-fold (bimodal) ^(b)

(a) As reported in Chiu and Ginsberg (2011), Tables S-6 through S-8.

(b) Values are presented for higher probability, upper mode.

In spite of the unresolved issues related to PCE's GST metabolism, OEHHA considers the Chiu and Ginsberg model to be the best available methodology for estimating dose metrics in the dose-response assessment. A simplified, deterministic version of the model was developed by identifying the main inhalation components, translating them from the MC Sim programming language into Berkeley Madonna code, and running the pared-down code in the usual deterministic manner. The optimized, Bayesian posterior mode parameters and other baseline values developed by Chiu and Ginsberg (2011) were used in the adapted model.

OEHHA's inhalation-only adaptation of the Chiu and Ginsberg model includes lung, liver, kidney, fat, and venous blood compartments, and lumped compartments for rapidly and slowly perfused tissues. The first transformation in the oxidative pathway is modeled in the lung, liver, and kidney, and the first step of the GST pathway is included for liver and kidney. Absorption-desorption of PCE in the upper respiratory tract (i.e., the "wash-in/wash-out" effect) is also included. The model adequately reproduced the predictions of the original Chiu and Ginsberg model for inhalation-only exposures. The Berkeley Madonna model code for mouse, rat, and human is provided in Appendix A.

7. GENOTOXICITY AND CARCINOGENICITY

Genotoxicity

A large number of studies have tested the genotoxicity of PCE, and less frequently its metabolites, in microorganisms, mammalian cells, and in *Drosophila* and rodents. There have also been a few occupational exposure studies looking at genetic abnormalities in lymphocytes. This literature has recently been reviewed in detail by IARC (2014) and U.S. EPA (2012a). Selected results based on these reviews and the literature are presented below.

PCE was not mutagenic in the Ames test with *S. typhimurium* or *E. coli* in the presence or absence of S9 metabolic activation. It was mutagenic, however, in *S. typhimurium* when tested with purified rat-liver GST, glutathione, and rat kidney fractions, where TCVG would be formed (Vamvakas, *et al.*, 1989). Most studies looking at chromosomal aberrations, micronuclei formation, or sister chromatid exchange have been negative, but micronuclei induction was seen in Chinese hamster ovary cells (Wang *et al.*, 2001) and human lymphoblastoid cells expressing CYP450 enzymes (White *et al.*, 2001). Genetic alterations have also been observed in rapidly growing yeast cell cultures (U.S. EPA, 2012a).

Other types of tests, such as DNA strand break assays, DNA adduct and cell transformation studies, and *Drosophila* mutation tests have provided mixed results. Positive findings include: Elevated DNA single-strand breaks in mouse liver and kidney *in vivo*, (Walles, 1986), and DNA-adduct formation in mouse and rat tissues *in vivo* (Mazzullo, *et al.*, 1987).

Results from occupational studies have also been mixed. Ikeda *et al.* (1980) tested ten factory workers exposed to high (92 ppm PCE) or low (10-40 ppm) and found no evidence of cytogenetic damage to lymphocytes or altered cell cycle kinetics. No increase in sister chromatid exchanges in lymphocytes was found in a study of 27 subjects exposed to 10 ppm (geometric mean) of PCE (Seiji *et al.*, 1990). A decrease (not increase) of 8-hydroxy-deoxyguanosine, a marker of oxidative DNA damage, was observed in leukocytes of 38 female dry cleaners exposed to average concentrations of less than 5 ppm PCE (Toraason *et al.*, 2003). On the other hand, a study of 18 dry-cleaning workers exposed to 3.8 ppm PCE (average) found evidence of short-term genetic damage to peripheral blood lymphocytes, indicated by an increase in acentric chromosomal fragments (Tucker *et al.*, 2011).

Genotoxicity testing of various PCE metabolites includes the following positive results:

- TCA exhibited genotoxicity in several *in vivo* tests, for example: DNA strand breaks, chromosomal abnormalities, and micronucleus formation in mice; and chromosomal aberrations in chicken bone marrow (IARC, 2014; U.S. EPA, 2012a).
- Genotoxicity has been demonstrated with DCA in the Ames test, micronucleus induction test, a mouse lymphoma assay, and *in vivo* cytogenetic tests; DCA has

also been shown to cause DNA strand breaks *in vivo* in mouse and rat liver (*ibid.*).

- Trichloroacetyl chloride vapor tested positive in the Ames test with and without metabolic activation (DeMarini, *et al.*, 1994).
- PCE epoxide was mutagenic without metabolic activation in the Ames test with *S. typhimurium* TA1535 at the lower doses tested; toxicity occurred at higher doses (Kline *et al.*, 1982).
- TCVG incubated with rat kidney protein containing γ -glutamyl transpeptidase (GGT) and dipeptidases was mutagenic in the Ames test (Vamvakas, *et al.*, 1989).
- TCVC and N-AcTCVC tested positive in the Ames test without metabolic activation (Dekant *et al.*, 1986; Vamvakas, *et al.*, 1987).
- TCVC sulfoxide was mutagenic in the Ames test with *S. typhimurium* TA 100, but was 30-fold less potent than TCVC (Irving and Elfarrar, 2013).

In addition, several metabolites have been tested for carcinogenicity in animals. Dermal exposure of mice to PCE epoxide induced skin tumors (Van Duuren, *et al.*, 1983). Several long-term drinking-water bioassays of TCA and DCA in mice, with limited pathologic analysis of tissues other than the liver, found increases in hepatocellular tumors. Initiation–promotion studies with TCA or DCA in mice also demonstrated that they promote liver tumors following initiation by other carcinogens (IARC, 2014; Guyton *et al.*, 2014).

Cancer Epidemiology

Numerous epidemiologic studies of PCE have been published, including more than 25 larger cohort and case-control studies since OEHHA's last toxicity review (*circa* 2000). Several detailed reviews of the literature have recently been published (Guyton, *et al.*, 2014; IARC, 2014; and U.S. EPA, 2012a).

Epidemiologic studies of PCE have all relied on semi-quantitative measures of exposure such as high/medium/low, ever/never exposed, or job categories. As such, the exposure data in this body of research is not of sufficient quality for use in quantitative dose-response analysis. However, it provides evidence that PCE causes cancer in humans and qualitatively supports the development of a unit risk value from animal studies. US EPA (2012a) evaluated the results of the cohort and case-control studies that developed more precise exposure assessments and concluded that PCE increases the risk of three types of cancer in humans: bladder cancer, non-Hodgkin's lymphoma (NHL), and multiple myeloma. IARC (2014) agreed with US EPA regarding bladder cancer, but concluded that the evidence for PCE inducing other cancers in humans was insufficient given the conflicting results across various studies. With non-Hodgkin's lymphoma, for example, "three cohort studies showed an increased risk based on small numbers, and the largest study with the best control of potential confounders did not. Case-control studies on non-Hodgkin lymphoma did not find significant associations" (*ibid.*).

A recent meta-analysis of bladder cancer risk in dry-cleaning workers (Vlaanderen, *et al.*, 2014), integrated the results of seven studies and 463 exposed cases, and found an overall relative risk level of about 1.5 for exposed versus non-exposed groups (with a 95% confidence level of 1.16 to 1.85).

Animal Studies of PCE

Increased tumor incidence was found in mice and rats in three long-term carcinogenicity studies of PCE. An oral study was conducted by the National Cancer Institute (NCI, 1977), where B6C3F1 mice and Osborne-Mendel rats were administered PCE in corn oil by gavage, 5 days/week for 78 weeks with additional follow-up of 32 weeks for rats and 12 weeks for mice. PCE caused a significant increase of hepatocellular carcinomas in mice of both sexes, and the tumors appeared considerably sooner in treated mice than in controls. Survival in the high dose groups was much lower than the control group at 40 to 45 weeks, and toxic nephropathy was observed in 93% of mice exposed. In rats, a high level of early mortality occurred in all treated groups, which obscured conclusions regarding carcinogenicity.

Two lifetime inhalation bioassays of PCE have also been published. NTP (1986) conducted a study where B6C3F1 mice and F344/N rats, in groups of 50, were exposed to PCE by inhalation, 6 hours/day, 5 days/week for 103 weeks. Mice were exposed to concentrations of 100 or 200 ppm, and rats to 200 or 400 ppm, in addition to controls. PCE significantly increased the rate of hepatocellular carcinomas in mice of both sexes. The combined incidence of liver adenoma or carcinoma was also significantly increased, although the incidence of liver adenomas separately was not. In female and male rats, PCE produced significant increases in mononuclear cell leukemia (MCL).

Male rats additionally exhibited an increase of renal tubular-cell adenomas and adenocarcinomas. Although the rate increases were not statistically significant, they appeared to be dose-related. Moreover, the historical incidence of these tumors is low (0.4%) at the laboratory and increased incidence has been found with other chlorinated ethanes and ethylenes. Thus renal tubular-cell tumors were judged to be related to PCE exposure. Brain glioma, another rare tumor type in F344 rats, was observed in one male control rat and in four male rats at 400 ppm exposure. This increase was not statistically significant. However, because the historical incidence of these tumors is 0.8% for the laboratory,² the increased brain tumor incidence in this study was also carried through the analysis.²

A second lifetime inhalation cancer study was conducted by the Japan Industrial Safety and Health Association (JISA, 1993) using F344/DuCrj rats and Crj:BDFr mice. Groups of 50 male and 50 female rats were exposed to PCE at 50, 200 or 600 ppm, and similar groups of mice were exposed to 10, 50, or 250 ppm, for 6 hours per day, 5 days per week, and 104 weeks. As in the NTP (1986) study, a significant increase in MCL was seen among male and female rats, and hepatocellular adenomas or carcinomas were elevated in mice of both sexes. Increased numbers of tumors were also found in the

² However, NTP (1986) concluded that brain gliomas were not related to PCE exposure.

harderian gland of male mice, as well as hemangioendotheliomas observed in all organs (but mostly in the spleen and liver).

Primary Studies for the Dose-Response Assessment

Both the NTP (1986) and JISA (1993) inhalation studies were judged to be of high quality and suitable for the development of an inhalation potency factor. The JISA dataset, however, offers the advantage of an additional dose category for each species, as well as the use of several lower exposure concentrations. Moreover, the control rate of MCL incidence in the F344/DuCrj rats used in the Japanese study (22 and 20%) was significantly lower than for the F344/N rats used in the NTP study (56 and 36%), and is expected to improve the precision of the fitted model. The NTP study, nonetheless, provides important additional data on tumor development in the kidney, brain, and testes of F344/N rats.

Based on the above considerations, OEHHA chose both the JISA (1993) and NTP (1986) bioassays as primary studies for the dose-response analysis. The dose-response data and results of statistical tests are presented in Tables 3 and 4. Given the availability of two acceptable inhalation studies, the oral NCI (1977) study was not used in the quantitative analysis.

Relevance of MCL to Humans

Some concerns about the propriety of using the rat MCL data for human risk assessment were raised by an NRC expert panel (without consensus) during a review of U.S. EPA's PCE IRIS evaluation (NRC 2010). One issue brought up by the panel was that MCL is a common tumor in aging F344 rats that lacks a corresponding tumor in humans. Panel members also questioned the statistical significance of the MCL dose-response data in light of the elevated historical and control-group incidence rates for MCL. This section briefly addresses both questions.

Regarding the issue of tumor-site concordance: Current research in cancer biology indicates that the basic cellular mechanisms of carcinogenesis are similar among mammals. However, this does not imply that exposure to a chemical carcinogen will always produce cancer in the same organ in different species (US EPA, 2005). In the case of human leukemias and lymphomas that are known to be induced by specific carcinogens, rodents develop different types of leukemia and lymphoma (U.S. EPA, 2012c). The sites of induced cancer may not be the same because of differing toxicokinetics and tissue susceptibilities. For leukemia and lymphoma, variation in susceptibility could be related to differences in hematopoiesis and immune surveillance. Accordingly, there is no expectation—in general or specifically for MCL—of tumor-site concordance when using animal studies to predict human cancer risk (OEHHA, 2009).

**Table 3: Primary Tumor Incidence in Mice and Rats Exposed to PCE
 Rates at Exposure Concentrations in PPM (JISA, 1993)**

Mice (Crj:BDFr)									
Tumor Type	Sex	Adjusted Rates ^{(a)(b)}				Rate Percent			
		0	10	50	250	0	10	50	250
Hepatocellular adenoma or carcinoma	M	13/46**	21/47	19/47	40/49**	28.3	44.7	40.4	81.6
	F	3/44**	3/41	7/40	33/46**	6.8	7.3	17.5	71.7
Hemangioma or hemangiosarcoma (All sites)	M	4/46*	2/47	7/47	9/49*	8.7	4.3	14.9	18.4
Harderian gland adenoma	M	2/41**	2/45	2/37	8/39	4.9	4.4	5.4	20.5

Rats (F344/DuCrj)									
Tumor Type	Sex	Adjusted Rates ^{(a)(b)}				Rate Percent			
		0	50	200	600	0	50	200	600
Mononuclear cell leukemia	M	11/50**	14/48	22/50	27/49*	22.0	29.2	44.0	55.1
	F	10/50 ^(c)	17/50	16/50	19/50	20.0	34.0	32.0	38.0

(a) Tumor-incidence denominator adjusted by excluding animals dying before the first corresponding tumor type observed in each study.

(b) Statistical test indicators: (*) P-value < 0.05; (**) P-value < 0.005. Fischer exact test results are as reported by JISA, except that mouse, all-site hemangioma/hemangiosarcoma values were calculated by OEHHA. The control group column indicates the results of trend tests. Both the Cochran-Armitage trend test (reported by JISA) and the exact trend test calculated by OEHHA gave the same indications of significance.

(c) A significant trend was found in a life-table test reported by JISA, P-value = 0.049.

**Table 4: Primary Tumor Incidence in Mice and Rats Exposed to PCE
 Rates at Exposure Concentrations in PPM (NTP, 1986)**

Mice (B6C3F1)							
Tumor Type	Sex	Adjusted Rates ^{(a)(b)}			Rate Percent		
		0	100	200	0	100	200
Hepatocellular adenoma or carcinoma	M	17/49**	31/47**	41/50**	34.7	70.0	82.0
	F	4/44**	17/42**	38/47**	9.1	40.5	80.9

Rats (F344/N)							
Tumor Type	Sex	Adjusted Rates ^{(a)(b)}			Rate Percent		
		0	200	400	0	200	400
Mononuclear cell leukemia	M	28/50*	37/48*	37/50*	56.0	77.1	74.0
	F	18/49*	30/50*	29/50*	36.1	60.0	58.0
Renal tubule adenoma or carcinoma	M	1/47 ^(c)	3/42	4/40	2.1	7.1	10.0
Brain glioma	M	1/44 ^(c)	0/37	4/35	2.3	0.0	11.4
Testicular interstitial cell	M	35/49 ^(c)	39/46	41/50	71.4	84.8	82.0

(a) Tumor-incidence denominator adjusted by excluding animals dying before the first corresponding tumor type observed in each study.

(b) Statistical test indicators: (*) P-value < 0.05; (**) P-value < 0.005. Fischer exact test results are as reported by NTP. The control group column indicates the results of trend tests. Both the Cochran-Armitage trend test (reported by NTP) and the exact trend test calculated by OEHHA gave the same indications of significance.

(c) Although testicular tumors and brain glioma did not appear to be significantly increased by the Fischer exact and trend tests, life table tests conducted by NTP did show a significant increase with trends of <0.001, and 0.039 respectively. The life table trend test for kidney was nearly significant at 0.054.

Notwithstanding this general principle, there is reasonable evidence that rat MCL corresponds to at least one form of human leukemia. The specific cell type and biological mechanisms that give rise to rat MCL are not known, but it appears to arise from a lymphocyte or monocyte lineage, and it is thought that the cell of origin resides in the spleen or undergoes neoplastic transformation in the spleen (Thomas et al., 2007). One reasonable hypothesis is that rat MCL is a form of Large Granular Lymphocyte Leukemia (LGLL), a cancer that develops in the spleen and is phenotypically and functionally similar to human LGLL (IARC, 1990; Thomas et al., 2007). Human LGLL derives from either T-cell or natural killer (NK) cell lineages (Sokol and Loughran, 2006). Additional support for linking rat MCL to human LGLL is provided by a study using the F344 rat MCL as a model for human NK-LGLL, which observed similar cellular responses in samples of the two tumor-cell types (Liao et al., 2011).

Exposure of humans and animals to relatively low doses of PCE produces adverse effects upon blood and the immune system (e.g., see: Marth, 1987; Kroneld, 1987; and Emara et al., 2010) that could plausibly give rise to a variety of carcinogenic response in different species. In addition to human LGLL, rat MCL may correspond to other types of human leukemia or lymphoma.

Regarding statistical issues arising from the elevated incidence of MCL in control groups: An NTP workshop focusing on the high background incidences of MCL and other tumors in the F344 rat noted that, "From a statistical perspective, high background rates of such tumors in control animals will generally decrease the ability to detect an exposure-related effect. In addition, when a statistically significant tumor effect is found in test animals relative to concurrent controls, the effect may not be considered exposure-related if it falls within the range observed in historical controls" (King-Herbert and Thayer, 2006). The foregoing statement focuses on the problem of false negative test results. However, since US EPA found MCL incidence to be significantly elevated in PCE-exposed rats, NRC panel members were concerned with the potential for false positive test results. On this issue, OEHHA agrees with the Massachusetts Department of Environmental Protection (MDEP), who reviewed the historical background rates of MCL in the NTP and JISA study laboratories and found that,

"For both the NTP (1986) and JISA (1993) studies, the background rate of MCL in the same study control group was greater than or equivalent to the historical control rates for the same lab, same sex. Thus, the controls in both studies did not exhibit anomalously low MCL, which could, had it occurred, lead to false positive responses in the treatment groups." (MDEP, 2014)

Indeed, for the JISA male rat MCL data, where the incidence in study controls was 22%, the historical incidence was 6-22%, and the Cochran-Armitage test for trend was highly significant, having a p-value of less than 0.0005.

8. MODE OF ACTION

PCE's carcinogenic mode of action (MOA) likely involves the genotoxicity of one or more of its oxidative- or GST-pathway metabolites, although the precise mechanisms are unknown.

Several PCE metabolites, e.g., PCE epoxide, oxalyl chloride, trichloroacetyl chloride, dichlorothioketene, and TCVC sulfoxide, are reactive compounds and expected to have short half-lives in the nucleophile-rich cellular environment.³ These substances will tend to react chemically and enzymatically with cellular components near their site of production. The relatively stable metabolites, such as: TCA, TCVC, N-AcTCVC, and the glutathione conjugate of TCVC sulfoxide, are more likely to circulate throughout the body where they may be further metabolized and impact tissues other than the liver and kidney.

Both trichloroacetic acid (TCA) and dichloroacetic acid (DCA) have independently been found to increase tumor formation in mice. Since TCA is a major metabolite of PCE, US EPA (2012a) evaluated whether it could be the primary source of PCE's carcinogenicity in mouse liver. Using dose-response data from the JISA (1993) and NTP (1986) PCE studies and a drinking water study of TCA in mice (DeAngelo, *et al.*, 2008), US EPA found that metabolically-generated TCA could contribute from 12 to 100 percent of the increased risk of liver tumors.

There are several non-genotoxic MOAs that may contribute to PCE's carcinogenicity, though in as yet poorly understood ways. These have been discussed at length by U.S. EPA (2012a), and include: cytotoxicity with subsequent cellular proliferation, oxidative stress-induced cellular transformation, and dysregulation due to altered DNA methylation. Two specific MOAs that are potentially relevant for evaluating PCE involve α 2u-globulin nephropathy in the male rat, and PPAR α activation⁴ for mouse liver tumors. In both cases, the biological bases for these MOAs in rodents are thought to be muted or absent in humans, indicating that the particular tumor-types may not be useful for human risk assessment.

α 2u-Globulin Nephropathy

The α 2u-globulin MOA in male rats is defined by: accumulation of α 2u-globulin-containing hyaline droplets in the proximal tubules of the kidney, cytotoxicity with tubular cell proliferation, exfoliation of epithelial cells into the proximal tubular lumen and formation of granular casts, papillary mineralization, hyperplastic foci, and renal tumors (U.S. EPA, 1991).

Green *et al.* (1990) found accumulation of α 2u-globulin in the proximal tubules of F344 rats exposed by inhalation to 1000 ppm of PCE for 10 days, or given 1500 mg/kg PCE by gavage for 42 days. However a 400 ppm inhalation exposure for 28 days did not produce protein droplets or other signs of toxicity. For chemicals known to cause α 2u-globulin toxicity, the formation of protein droplets in the kidney occurs rapidly upon exposure (frequently after a single dose), and further indications of tissue damage begin to appear in 3 to 4 weeks (Lehman-McKeeman, 2010; Green *et al.*, 1990). Thus, the absence of α 2u-globulin accumulation after a 28-day exposure suggests that 400 ppm of PCE will not result in α 2u-globulin toxicity upon long-term exposures.

³ For example, the high reactivity of PCE epoxide is indicated by its 2.6-minute half-life in a neutral aqueous buffer solution at 37 °C (Yoshioka, *et al.*, 2002).

⁴ PPAR α = "peroxisome proliferator-activated receptor- α ."

The NTP (1986) study provided additional evidence along these lines. Karyomegaly and cytomegaly were observed in the kidneys of rats exposed to 200 or 400 ppm for 2 years, but indicators of α 2u-globulin nephropathy (e.g., hyaline droplets, mineralization, and cast formation) were not found. The NTP protocol at the time was not designed to detect hyaline droplets or α 2u-globulin accumulation (U.S. EPA 2012a) but would have observed other markers of α 2u-globulin toxicity if this MOA had been in effect. Moreover, comparable toxicity was observed in female rats in the NTP study, and PCE caused similar kidney damage in rats and mice of both sexes in the NCI (1977) gavage study. This suggests that PCE's nephrotoxicity is neither sex nor species specific, as would be expected with an α 2u-globulin MOA.

PPAR α Activation

The PPAR α MOA involves activation of the PPAR α nuclear receptor, which is hypothesized to cause alterations in cell proliferation and apoptosis, and clonal expansion of initiated cells. The proposed indicators for this mode of action are: (1) PPAR α activation with associated peroxisome proliferation, or (2) PPAR α -activation plus increased liver weight and effects such as increased peroxisomal β -oxidation, CYP4A, or acyl CoA oxidase (Klaunig, et al., 2003).

Numerous studies have been carried out to verify the PPAR α MOA. The evidence obtained from this body of research has been mixed, and it currently remains unclear whether this hypothetical MOA is a major causal factor in mouse-liver tumor formation. The U.S. EPA has published several detailed reviews of the PPAR α MOA in its IRIS program toxicity reviews for PCE and TCA (U.S. EPA 2012a, 2011). The main conclusions of these reviews are:

- PPAR α activators can produce multiple effects in addition to peroxisome proliferation, including genotoxicity, oxidative stress, hypomethylation of DNA, and activation of other nuclear receptors.
- Peroxisome proliferation and the associated markers of PPAR α activation are poor predictors of hepatocarcinogenesis in mice and rats. Studies with various PPAR α activators show that the correlation between *in vitro* PPAR α activation potency and tumorigenesis is weak and this relationship does not appear to be due to differences in pharmacokinetics. This suggests the involvement of carcinogenic mechanisms other than PPAR α -activation.
- Studies of the PPAR α -agonist, diethyl hexyl phthalate (DEHP) in transgenic mouse strains, although not fully conclusive, have cast doubt on whether the key events in the PPAR α MOA (receptor activation, hepatocellular proliferation, and clonal expansion) are sufficient to cause liver tumors. The studies suggest that DEHP can induce tumors in a PPAR α -independent manner (Ito *et al.*, 2007a), and that PPAR α activation in hepatocytes is insufficient to cause tumorigenesis (Yang *et al.*, 2007). This again indicates that other mechanisms, either independently or in combination with PPAR α -activation, are necessary to induce tumors.

- PCE exposure leads to PPAR α -activation and modest levels of peroxisome proliferation, predominantly through its metabolite TCA. There is conflicting evidence as to whether this causes cellular proliferation in animals exposed to PCE: the peroxisome proliferation caused by PCE lacks specificity and consistency with respect to tissue, species, dose, and sequence of events. Also, there is little evidence indicating that PCE can induce clonal expansion of initiated cells. The available information for PCE is insufficient to demonstrate that the PPAR α MOA plays a significant causative role in mouse hepatocarcinogenesis.

Conclusion on PCE's Mode of Action

Given the limited understanding of the various non-genotoxic MOAs that may modify or add to the tumorigenic effects of PCE's genotoxic metabolites, there are insufficient grounds to evaluate PCE as primarily a non-genotoxic carcinogen using a non-linear model.

9. DOSE-RESPONSE ASSESSMENT

Dose Metrics

Much of the following information has already been presented, but is briefly restated here because of its relevance to choosing metrics for the dose-response calculations:

- The liver is the main site of oxidative PCE-metabolite formation, but other tissues with CYP 450 2E1, 2B, and 3A activity may also contribute to the oxidative-pathway. TCA is a relatively stable metabolite that has been found to increase liver tumors in mice via oral exposure. TCA's cancer potency in other tissues has not been adequately examined.
- Of the two metabolic pathways, oxidation is the main pathway in rodents. For example, at 10 ppm exposure, the PBPK model indicates that the ratio of oxidation to glutathione conjugation is 600 in mice and 19.5 in rats.
- Saturation of the oxidative pathway begins to occur between 1 and 10 ppm exposure in mice, and between 10 and 100 ppm exposure in rats (see Table 2). Saturation causes the ratio of oxidized to absorbed PCE to decrease at higher exposure concentrations. The smaller amount of metabolism that occurs via the GST pathway, on the contrary, increases somewhat at higher exposure concentrations in rodents.
- Although most GST conjugation of PCE takes place in the liver, the kidney is the main site for production of reactive GST-pathway metabolite dichlorothioketene. Other metabolites such as: TCVC, N-AcTCVC, and TCVC sulfoxide (and its glutathione conjugate) are formed in both the kidney and liver, and may circulate to other metabolizing tissues as well.
- It is not known which PCE metabolites, or even which of the two main metabolic pathways produces the most carcinogenic risk.
- The PBPK model for the GST pathway in humans involves a large variability or uncertainty, with two possible values (posterior modes) for the rate of PCE conjugation that differ by a factor of approximately 3000. It is not known how much

of the model variability is due to the wide range of GST activities that has been observed in the human population, but it is reasonable to assume that some segment of the population could be very efficient metabolizers. The more probable and larger of the two values indicates that glutathione conjugation predominates over oxidation in humans, the ratio of PCE conjugation to oxidation being about 10.

Given the uncertainties underlying the toxicokinetics and toxicodynamics of PCE, several reasonable dose metrics could be used, each having analytical strengths and weaknesses:

- Total PCE metabolism, which consists of the sum of oxidative and GST pathway metabolism in the liver and kidney, plus oxidation in the lung
- Pathway-specific metabolism, i.e., using either oxidative- or GST-pathway metabolism separately for one or more tissues
- PCE blood concentration, i.e., area under the concentration curve (AUC), and
- Applied air concentration

Using total metabolism for the dose metric accounts for known metabolic differences across species and provides a dose adjustment for saturation effects in the oxidative pathway, but it also involves assuming that carcinogenic potency is directly proportional to the rates of metabolite production in the two pathways. The use of pathway-specific metabolism, on the other hand, would be based on assuming that one pathway dominates the carcinogenic potency in one or more tissues. Using either PCE AUC or applied concentration as the dose metrics discounts much of the species-specific metabolic information provided by the PBPK model.

Considering all of the above factors, total metabolism was chosen as the best general metric for the dose-response analysis. The PBPK-estimated, metabolized doses used in the dose-response analysis are presented in Appendix B.

Dose-Response Model

Since PCE is considered to be a genotoxic carcinogen, the dose-response relationship was assumed to approach linearity at low doses and the multistage cancer model was chosen to estimate the potency factor. This is consistent with OEHHA risk assessment guidelines which indicate that use of the multistage model (plus low-dose linearity) is reasonable under such circumstances (OEHHA, 2009). In the traditional multistage model, cancer potency is estimated as the upper 95% confidence bound, (q_1^*), on the linear coefficient (q_1) in the following expression relating lifetime probability of cancer (p) to dose (d):

$$p = q_0 + (1 - q_0)(1 - \exp[-(q_1d + q_2d^2 + \dots)])$$

In the above equation, (d) represents the average daily dose resulting from a uniform, continuous exposure over the nominal lifetime of the animal (two years for both mice and rats). For studies where the exposures vary in time, they are averaged over the entire study period and modeled as if they were uniform and continuous. Prior to fitting the dose-response model to the study data, an adjustment is made to the incidence rates to account

for inter-current mortality, which decreases the pool of animals at risk of developing tumors throughout the study.

The latest version of BMDS (Version 2.6.0.1, US EPA, 2015) was used to carry out the necessary dose-response calculations. The BMDS dichotomous multi-stage cancer model was run for all allowed degrees of the approximating polynomial, with a benchmark risk (BMR) of 5 percent. The software calculates benchmark doses (BMDs) and their 95% lower confidence levels (BMDLs). When multiplied by the BMR, the reciprocal of the BMDL gives a unit risk factor that is generally close in value to, and is used in place of (q_1^*). For each tumor site, the model with the lowest value of AIC (Akaike's Information Criterion) was chosen, as long as its p-value for goodness-of-fit was above 0.1 and the absolute value of the scaled residual for the dose near the BMD was less than 2.0. The optimal model typically resulted from fitting a polynomial of 1 or 2 degrees, and the models with the lowest AIC also had the highest p-values (signifying the best fit to the data).

Interspecies extrapolation from experimental animals to humans was based on body weights (bw) raised to three-quarters power (U.S. EPA, 2005; Anderson *et al.*, 1983), which for BMDLs, may be expressed in terms of body weight raised to one-quarter power, as follows:

$$BMDL_{(Human)} = BMDL_{(Animal)} \times \left(\frac{bw_{(Animal)}}{bw_{(Human)}} \right)^{1/4}$$

The above equation is presumed to account for the toxicokinetic and toxicodynamic differences between species. Toxicokinetic modeling can sometimes eliminate the need for toxicokinetic scaling between animals and humans. This would be the case, for example, if the dose metric used in the analysis was the AUC of a directly carcinogenic metabolite. The remaining toxicodynamic differences would then be addressed, according to OEHHA practice, by scaling according to the one-eighth power of the body weight ratio.⁵ Using the rate of PCE metabolism as a dose metric, on the other hand, does not account for the toxicokinetics of other downstream biological processes that determine tissue concentrations of the relevant carcinogenic species. In this case, the full cross-species scaling factor is used (U.S. EPA, 1992).

Since PCE induced tumors at multiple sites in male mice (JISA study) and male rats (NTP study), the combined cancer potency was also estimated for these groups using the multi-site tumor module provided in BMDS. The BMDS procedure for summing risks over several tumor sites uses the profile likelihood method. In this method, the maximum likelihood estimates (MLEs) for the multistage model parameters (q_i) for each tumor type are added together (*i.e.*, $\sum q_0, \sum q_1, \sum q_2$), and the resulting model is used to determine a combined BMD. Then a confidence interval for the combined BMD is calculated by computing the desired percentile of the chi-squared distribution associated with a likelihood ratio test having one degree of freedom.

Once the organ-specific and multi-site BMDLs were obtained and scaled by body-weight, the toxicokinetic model was used to estimate the continuous 24-hour air concentration that

⁵ US EPA risk assessment guidelines (2005) suggest "retaining some of the cross-species scaling factor (e.g., using the square root of the cross-species scaling factor)," when toxicokinetic modeling is used without toxicodynamic modeling.

would produce the same daily metabolized dose for an adult human (i.e., the human equivalent concentration or "HEC"). The cancer potency values were then calculated by dividing the BMR of 0.05 by the HEC. Table 5 provides the calculated BMDs, BMDLs, and the interspecies-adjusted BMDLs for individual and combined tumor sites. Potency values derived from the primary studies are presented in Table 6 as unit risks factors (URFs) with units of reciprocal $\mu\text{g}/\text{m}^3$.

Inhalation Potency Value for PCE

The updated carcinogenic potency value for PCE is based on the following observations and rationale:

- Tissue-specific URF values calculated from the JISA study are of similar magnitude to the corresponding URFs obtained from the NTP study, though somewhat lower. For mouse liver tumors, the ratio of the JISA UR to the NTP UR was about 0.8 in both females and males. For rat MCL the corresponding ratios were 0.4 for females and 0.6 for males. The smaller URF values from the JISA data may be due in part to the higher precision obtained by the study having used lower doses and an additional dose group.
- In both studies, the males of both species appeared to be more sensitive than the corresponding females to the tumorigenic effects of PCE.
- The URF values from both studies ranged from 2.8E-06 to 1.6E-05 (per $\mu\text{g}/\text{m}^3$), within a factor of 6. (The compared values included the multi-tumor risks for male NTP rats and male JISA mice, as well as tissue-specific risks for other organs in mice and rats of both sexes.) Looking only at males of each species, the URFs ranges from 4.0E-06 to 1.6E-05.
- The highest URF was obtained from the combined site (i.e., multi-tumor) risk in male rats in the NTP study. This value was obtained by including MCL, brain, testicular, and renal tumors in the multi-tumor calculation.
- The URF values for mouse liver tumors and rat MCL were judged by OEHHHA to be more certain in view of the qualitative and quantitative agreement between the two primary studies; mouse liver tumors were also found in the NCI (1977) oral exposure study.
- The unique tumors seen in the NTP study, including kidney tumors, are important to consider. The kidney is one site where the GST-pathway may contribute substantially to the cancer potency. Moreover, there is reasonable evidence that the GST-pathway may also contribute to tumorigenesis in other organ systems.
- Although it appears likely that PCE exposure increased the rate of testicular tumors in rats, the relatively high risk value obtained for testicular tumors in NTP rats may be more uncertain, given the high tumor incidence seen in the control group (71%).

Considering the above points, and also that the set of calculated values is clustered in a narrow range, the geometric mean of the male mouse and rat URFs from both studies was chosen as the best estimate of PCE cancer potency. Specifically, the geometric mean was calculated using the following URF values:

Species	Study	URF
Male Mouse	JISA (Multiple tumor)	4.02E-06
	NTP (Liver)	4.44E-06
Male Rat	JISA (MCL)	4.81E-06
	NTP (Multiple tumor)	1.57E-05
	Geometric Mean	6.06E-06

The resulting URF, when rounded to two significant figures, is 6.1E-06 (per $\mu\text{g}/\text{m}^3$). A cancer slope factor of 2.1E-02 (per mg/kg-day) was also calculated from the URF by assuming a 70 (kg) adult breathes 20 (m^3/day) of air.

Table 5: BMD5 Modeling Results for the Primary Studies

Study	Sex	Tumor Type	P-value for multi-stage model fit	Scaled residual for dose near the BMD	BMD (mg/kg-day)	BMDL (mg/kg-day)	Animal BW (kg)	BW-Scaled BMDL (mg/kg-day)
Results from Mouse Studies								
JISA	M	Hepatocellular adenoma or carcinoma	0.22	1.17	3.06	2.16	0.048	0.350
		Harderian gland	0.99	-0.06	38.56	12.34	0.048	1.997
		Hemangioma or Hemangiosarcoma	0.35	0.94	26.61	12.98	0.048	2.100
		Combined site			2.73	1.85	0.048	0.300
	F	Hepatocellular adenoma or carcinoma	0.77	-0.23	10.33	3.84	0.035	0.574
NTP	M	Hepatocellular adenoma or carcinoma	0.85	0.03	2.46	1.79	0.037	0.272
	F	Hepatocellular adenoma or carcinoma	0.82	0.05	11.27	3.15	0.025	0.432
Results from Rat Studies								
JISA	M	Mononuclear cell leukemia	0.79	0.07	1.34	0.89	0.45	0.251
	F	Mononuclear cell leukemia	0.37	1.05	3.99	1.84	0.30	0.472
NTP	M	Mononuclear cell leukemia	0.23	-0.31	0.92	0.51	0.44	0.144
		Testicular interstitial cell	0.35	-0.26	1.06	0.48	0.44	0.136
		Renal adenoma or carcinoma	0.93	0.07	6.76	3.24	0.44	0.913
		Brain glioma	0.15	0.62	9.45	5.07	0.44	1.426
		Combined site			0.46	0.28	0.44	0.078
	F	Mononuclear cell leukemia	0.25	-0.30	1.24	0.72	0.32	0.188

Table 6: Unit Risk Factors from Primary Studies

Study	Sex	Tumor Type	BW-Scaled BMDL (mg/kg-day)	HEC based on PBPK Model (ppm)	Unit Risk Factor (URF) per ug/m ³
Results from Mouse Studies					
JISA	M	Hepatocellular adenoma or carcinoma	0.350	2.14	3.5E-06
		Harderian gland	1.997	12.20	6.0E-07
		Hemangioma or Hemangiosarcoma	2.100	12.83	5.7E-07
		Combined site	0.300	1.83	4.0E-06
	F	Hepatocellular adenoma or carcinoma	0.574	3.51	2.1E-06
NTP	M	Hepatocellular adenoma or carcinoma	0.272	1.66	4.4E-06
	F	Hepatocellular adenoma or carcinoma	0.432	2.64	2.8E-06
Results from Rat Studies					
JISA	M	Mononuclear cell leukemia	0.251	1.53	4.8E-06
	F	Mononuclear cell leukemia	0.472	2.88	2.6E-06
NTP	M	Mononuclear cell leukemia	0.144	0.88	8.4E-06
		Testicular interstitial cell	0.136	0.83	8.9E-06
		Renal adenoma or carcinoma	0.913	5.57	1.3E-06
		Brain glioma	1.426	8.71	8.5E-07
		Combined site	0.078	0.47	1.6E-05
	F	Mononuclear cell leukemia	0.188	1.15	6.4E-06

10. REFERENCES

- Anders MW, Lash L, Dekant W, Elfarra AA, Dohn DR, Reed DJ. 1988. Biosynthesis and biotransformation of glutathioneS-Conjugates to toxic metabolites. *CRC Critical Reviews in Toxicology* 18:311-341.
- Anderson EL. 1983. Quantitative Approaches in Use to Assess Cancer Risk. *Risk Analysis* 3:277-295.
- ARB. 2012. California Environmental Protection Agency, Air Resources Board, Air Toxic Emissions Inventory, 2012.
- Birner G, Richling C, Henschler D, Anders MW, Dekant W. 1994. Metabolism of tetrachloroethene in rats: identification of N epsilon-(dichloroacetyl)-L-lysine and N epsilon-(trichloroacetyl)-L-lysine as protein adducts. *Chemical Research in Toxicology* 7:724-732.
- Bull RJ, Sasser LB, Lei XC. 2004. Interactions in the tumor-promoting activity of carbon tetrachloride, trichloroacetate, and dichloroacetate in the liver of male B6C3F1 mice. *Toxicology* 199:169-183.
- CDHS. 1991. California Department of Health Services. Health Effects of Tetrachloroethylene (PCE). Berkeley, CA.
- Chiu WA, Ginsberg GL. 2011. Development and evaluation of a harmonized physiologically based pharmacokinetic (PBPK) model for perchloroethylene toxicokinetics in mice, rats, and humans. *Toxicology and Applied Pharmacology* 253:203-234.
- Clewell HJ, Gentry PR, Kester JE, Andersen ME. 2005. Evaluation of physiologically based pharmacokinetic models in risk assessment: An example with perchloroethylene. *Critical Reviews in Toxicology* 35:413-433.
- Dallas CE, Chen XM, O'Barr K, Muralidhara S, Varkonyi P, Bruckner JV. 1994. Development of a physiologically based pharmacokinetic model for perchloroethylene using tissue concentration-time data. *Toxicol Appl Pharmacol* 128: 50-59.
- DeAngelo A B, Daniel FB, Wong DM, George MH. 2008. The induction of hepatocellular neoplasia by trichloroacetic acid administered in the drinking water of the male B6C3F1 mouse. *J Toxicol Environ Health A*71:1056-1068.
- Dekant W. 1986. Metabolic conversion of tri- and tetrachloroethylene: formation and deactivation of genotoxic intermediates. *Dev Toxicol Environ Sci* 12:211-221.
- Dekant W, Metzler M, Henschler D. 1986. Identification of S-1,2,2-trichlorovinyl-N-acetylcysteine as a urinary metabolite of tetrachloroethylene: bioactivation through glutathione conjugation as a possible explanation of its nephrocarcinogenicity. *J Biochem Toxicol*. 1986. 1(2):57-72.
- Dekant W, Martens G, Vamvakas S, Metzler M, Henschler D. 1987. Bioactivation of tetrachloroethylene: role of glutathione S-transferase-catalyzed conjugation versus Cytochrome P-450-dependent phospholipid alkylation. *Drug Metabolism and Disposition* 15:702-709.

DeMarini DM, Perry E, Shelton ML. 1994. Dichloroacetic acid and related compounds: induction of prophage in *E. coli* and mutagenicity and mutation spectra in *Salmonella* TA100. *Mutagenesis* 9(5): 429-437.

Dow. 2008. The Dow Chemical Company. Product Safety Assessment, Perchloroethylene. June 24, 2008.

Emara AM, Abo El-Noor MM, Hassan NA, Wagih AA. 2010. Immunotoxicity and hematotoxicity induced by tetrachloroethylene in egyptian dry cleaning workers. *Inhalation Toxicology* 22:117-124.

Fernandez J, Guberan E, Caperos J. 1976. Experimental human exposures to tetrachloroethylene vapor and elimination in breath after inhalation. *Am Ind Hyg Assoc J* 37:143-150.

Frantz SW, Watanabe PG. 1983. Tetrachloroethylene: balance and tissue distribution in male Sprague-Dawley rats by drinking-water administration. *Toxicology and Applied Pharmacology* 69:66-72.

Green T, Odum J, Nash JA, Foster JR. 1990. Perchloroethylene-induced rat kidney tumors: an investigation of the mechanisms involved and their relevance to humans. *Toxicology and Applied Pharmacology* 103:77-89.

Guyton KZ, Chiu WA, Bateson TF, Jinot J, Scott CS, Brown RC, Caldwell JC. 2009. A reexamination of the PPAR- α activation mode of action as a basis for assessing human cancer risks of environmental contaminants. *Environ Health Perspect* 117:1664-1672.

Guyton KZ, et al. 2014. Human health effects of tetrachloroethylene: key findings and scientific issues. *Environ Health Perspect* 122:325-334.

Hannon-Fletcher MP, Barnett YA. 2008. Lymphocyte cytochrome P450 expression: inducibility studies in male Wistar rats. *Br J Biomed Sci* 65:1-6.

Hinchman CA, Ballatori N. 1994. Glutathione conjugation and conversion to mercapturic acids can occur as an intrahepatic process. *J Toxicol Environ Health* 41:387-409.

HSDB. 2010. Hazardous Substance Data Bank. National Library of Medicine, Bethesda MD. (Internet version accessed in 2015).

IARC. 1990. International Agency for Research on Cancer. Pathology of Tumors in Laboratory Animals, 1: Tumours of the Rat. IARC Scientific Publication, No. 99, 2nd edition, Lyon France.

IARC. 2014. International Agency for Research on Cancer. Trichloroethylene, tetrachloroethylene, and some other chlorinated agents / IARC Working Group on the Evaluation of Carcinogenic Risks to Humans (2012: Lyon, France). IARC monographs on the evaluation of carcinogenic risks to humans. Vol 106.

Ikeda M, Koizumi A, Watanabe T, Endo A, Sato K. 1980. Cytogenetic and cytokinetic investigations on lymphocytes from workers occupationally exposed to tetrachloroethylene. *Toxicology Letters* 5(3-4): 251-256.

Irving RM, Elfarra AA. 2012. Role of reactive metabolites in the circulation in extrahepatic toxicity. *Expert Opin Drug Metab Toxicol* 8:1157-1172.

Irving RM, Elfarra AA. 2013. Mutagenicity of the cysteine S-conjugate sulfoxides of trichloroethylene and tetrachloroethylene in the Ames test. *Toxicology* 306:157-161.

Ito Y, et al. 2007. Di(2-ethylhexyl)phthalate induces hepatic tumorigenesis through a peroxisome proliferator-activated receptor alpha-independent pathway. *J Occup Health* 49:172-182.

JISA. 1993. Japan Industrial Safety and Health Association, Japan Bioassay Research Center. Carcinogenicity study of tetrachloroethylene by inhalation in rats and mice. 2445 Hirasawa, Hadano, Kanagawa, 257-0015, Japan. March .31, 1993.

King-Herbert, Thayer. 2006. NTP workshop: Animal model for the NTP rodent Cancer bioassay: Strain and Stock-Should we Switch? *Toxicol Pathol*, 34: 802-805.

Klaunig JE, et al. 2003. PPARalpha agonist-induced rodent tumors: Modes of action and human relevance. *Critical Reviews in Toxicology* 33:655-780.

Kline SA, McCoy EC, Rosenkranz HS, Van Duuren BL. 1982. Mutagenicity of chloroalkene epoxides in bacterial systems. *Mutat Res* 101:115-125.

Kroneld R. 1987. Effect of volatile halocarbons on lymphocytes and cells of the urinary tract. *Bull Environ Contam Toxicol* 38:856-861.

Lash LH, Lipscomb JC, Putt DA, Parker JC. 1999. Glutathione conjugation of trichloroethylene in human liver and kidney: kinetics and individual variation. *Drug Metabolism and Disposition* 27:351-359.

Lash LH, Parker JC. 2001. Hepatic and Renal Toxicities Associated with Perchloroethylene. *Pharmacological Reviews* 53:177-208.

Lehman-McKeeman, LD. 2010. 2u-Globulin Nephropathy, in McQueen, C. A., *Comprehensive toxicology*. 2nd ed. / Oxford: Elsevier, 2010.

Liao A, et al. 2011. Therapeutic efficacy of FTY720 in a rat model of NK-cell leukemia. *Blood* 118:2793-2800.

Marth E. 1987. Metabolic changes following oral exposure to tetrachloroethylene in subtoxic concentrations. *Archives of Toxicology* 60:293-299.

Mazzullo M, Grilli S, Lattanzi G, Prodi G, Turina MP, Colacci A. 1987. Evidence of DNA binding activity of perchloroethylene. *Res Commun Chem Pathol Pharmacol* 58:215-235.

MDEP. 2014. Massachusetts Department of Environmental Protection, Office of Research and Standards, Tetrachloroethylene (Perchloroethylene), Inhalation Unit Risk Value, June 25, 2014.

NCI. 1977. National Cancer Institute. Bioassay of tetrachloroethylene for possible carcinogenicity. Bethesda, Md: National Institutes of Health. Report no. NCI-CGTR-13; DHEW Publication No. (NIH) 77-813.

NRC. 2010. National Research Council. Review of the Environmental Protection Agency's draft IRIS assessment of tetrachloroethylene. National Academies Press.

NTP. 1986. National Toxicology Program, U.S. Department of Health and Human Services. Toxicology and carcinogenesis studies of tetrachloroethylene (perchloroethylene) (CAS no. 127-18-4) in F344/N rats and B6C3F1 mice (inhalation studies). Research Triangle Park, NC. NTP Report no. TR 311.

NTP. 2014. National Toxicology Program, U.S. Department of Health and Human Services. National Institutes of Health. 13th Report on Carcinogens. October 2, 2014.

Odum J, Green T, Foster JR, Hext PM. 1988. The role of trichloroacetic acid and peroxisome proliferation in the differences in carcinogenicity of perchloroethylene in the mouse and rat. *Toxicology and Applied Pharmacology* 92:103-112.

OEHHA. 1992. Office of Environmental Health Hazard Assessment, California Environmental Protection Agency. Health Effects of Perchloroethylene. May, 1992.

OEHHA. 2001. Office of Environmental Health Hazard Assessment, California Environmental Protection Agency. Public Health Goal for Tetrachloroethylene in Drinking Water. August, 2001.

OEHHA. 2009. Office of Environmental Health Hazard Assessment, California Environmental Protection Agency. Technical Support Document for Cancer Potency Factors, Methodologies for derivation, listing of available values, and adjustments to allow for early life stage exposures. May 2009.

OEHHA. 2012. Office of Environmental Health Hazard Assessment, California Environmental Protection Agency. Technical Support Document for Exposure Assessment and Stochastic Analysis. August 2012.

Ohtsuki T, Sato K, Koizumi A, Kumai M, Ikeda M. 1983. Limited capacity of humans to metabolize tetrachloroethylene. *Int Arch Occup Environ Health* 51:381-90.

Reddy MB. 2005. Physiologically based pharmacokinetic modeling: science and applications. Wiley-Interscience.

Rooseboom M, Vermeulen NP, Groot EJ, Commandeur JN. 2002. Tissue distribution of cytosolic beta-elimination reactions of selenocysteine Se-conjugates in rat and human. *Chemico-Biological Interactions* 140:243-264.

Seiji K, Jin C, Watanabe T, Nakatsuka H, Ikeda M. 1990. Sister chromatid exchanges in peripheral lymphocytes of workers exposed to benzene, trichloroethylene, or tetrachloroethylene, with reference to smoking habits. *Int Arch Occup Environ Health* 62:171-176.

Sokol L, Loughran TP, Jr. 2006. Large granular lymphocyte leukemia. *Oncologist* 11:263-273.

Thomas J, Haseman JK, Goodman JI, Ward JM, Loughran TP, Jr., Spencer PJ. 2007. A review of large granular lymphocytic leukemia in Fischer 344 rats as an initial step toward evaluating the implication of the endpoint to human cancer risk assessment. *Toxicol Sci* 99:3-19.

Toraason M, et al. 2003. Effect of perchloroethylene, smoking, and race on oxidative DNA damage in female dry cleaners. *Mutation Research/Genetic Toxicology and Environmental Mutagenesis* 539:9-18.

Tucker JD, Sorensen KJ, Ruder AM, McKernan LT, Forrester CL, Butler MA. 2011. Cytogenetic analysis of an exposed-referent study: perchloroethylene-exposed dry cleaners compared to unexposed laundry workers. *Environ Health* 10:16.

USEPA. 1991. Alpha-2u-globulin: Association with chemically induced renal toxicity and neoplasia in the male rat. Washington, DC: U.S. Environmental Protection Agency, National Center for Environmental Assessment. Report no. EPA/625/3-91/019F.

USEPA. 1992. Draft report: A cross-species scaling factor for carcinogen risk assessment based on equivalence of mg/kg(3/4)/day. *Federal Register* 57:24151-24173.

USEPA. 2005. U.S. Environmental Protection Agency. Guidelines for carcinogen risk assessment. Risk Assessment Forum. Report no. EPA/630/P-03/001F.

US EPA. 2011. U.S. Environmental Protection Agency. Toxicological Review of Trichloroacetic Acid, In Support of Summary Information on the Integrated Risk Information System (IRIS), Report no. EPA/635/R-09/003F.

US EPA. 2012a. U.S. Environmental Protection Agency. Toxicological Review of Tetrachloroethylene (Perchloroethylene), In Support of Summary Information on the Integrated Risk Information System (IRIS). Report no. EPA/635/R-08/011F.

US EPA. 2012b. U.S. Environmental Protection Agency. Integrated Risk Information System (IRIS) Chemical Assessment Summary: Tetrachloroethylene (Perchloroethylene).

US EPA. 2012c. U.S. Environmental Protection Agency. Lymphohematopoietic Cancers Induced by Chemicals and Other Agents: Overview and Implications for Risk Assessment, EPA/600/R-10/095F.

US EPA. 2015. U.S. Environmental Protection Agency, National Center for Environmental Assessment. Benchmark Dose Software (BMDS) Version 2.6.0.1.

Vamvakas S, Dekant W, Berthold K, Schmidt S, Wild D, Henschler D. 1987. Enzymatic transformation of mercapturic acids derived from halogenated alkenes to reactive and mutagenic intermediates. *Biochemical Pharmacology* 36:2741-2748.

Vamvakas S, Dekant W, Henschler D. 1989a. Genotoxicity of haloalkene and haloalkane glutathione S-conjugates in porcine kidney cells. *Toxicology in Vitro* 3:151-156.

Vamvakas S, Herkenhoff M, Dekant W and Henschler D. 1989b. Mutagenicity of tetrachloroethene in the ames test—metabolic activation by conjugation with glutathione. *J Biochem Toxicol* 4:21–27.

Van Duuren BL, Kline SA, Melchionne S, Seidman I. 1983. Chemical structure and carcinogenicity relationships of some chloroalkene oxides and their parent olefins. *Cancer Res* 43:159-162.

Vlaanderen J, et al. 2014. Tetrachloroethylene exposure and bladder cancer risk: a meta-analysis of dry-cleaning-worker studies. *Environ Health Perspect* 122:661-666.

Walles SA. 1986. Induction of single-strand breaks in DNA of mice by trichloroethylene and tetrachloroethylene. *Toxicology Letters* 31:31-35.

Wang JL, Chen WL, Tsai SY, Sung PY, Huang RN. 2001. An in vitro model for evaluation of vaporous toxicity of trichloroethylene and tetrachloroethylene to CHO-K1 cells. *Chemico-Biological Interactions* 137:139-154.

White IN, Razvi N, Gibbs AH, Davies AM, Manno M, Zaccaro C, De Matteis F, Pahler A, Dekant W. 2001. Neoantigen formation and clastogenic action of HCFC-123 and perchloroethylene in human MCL-5 cells. *Toxicology Letters* 124:129-138.

Yang Q, Ito S, Gonzalez FJ. 2007. Hepatocyte-restricted constitutive activation of PPAR alpha induces hepatoproliferation but not hepatocarcinogenesis. *Carcinogenesis* 28:1171-1177.

Yoshioka T, Krauser JA, Guengerich FP. 2002. Tetrachloroethylene oxide: hydrolytic products and reactions with phosphate and lysine. *Chemical Research in Toxicology* 15:1096-1105.

APPENDIX A

**PBPK Model Code for Simplified, Inhalation-Only Adaptation of Chiu and Ginsberg
(2011) PCE Model, for Mice, Rats, and Humans
(Written in Berkeley Madonna)**

{ Inhalation-Only Adaptation of Chiu and Ginsberg (2010) PCE Model
for MICE }

```
METHOD RK4
STARTTIME = 0
STOPTIME=504
DT = 0.002

ppm=10      {inhaled conc in ppm}
Cinh=If (Mod(Time,24)<=6 AND Mod(Time,168)<=120) Then (ppm*165.83/24450) Else 0

; BW=0.037 {NTP Male}
; BW=0.048 {JISA Male}
; BW=0.025 {NTP Female}
  BW=0.035 {JISA Female}

QC=11.6*BW^0.75
QP=QC*2.5*exp(0.325015)
QM=QP/0.7    {minute volume, L/h}
DResp=QP*exp(0.203)
; Intake=QM*Cinh*24/BW

QGut=0.141*QC
QLiv=0.02*QC
QKid=0.091*QC
QFat=0.07*QC
QRap=0.461*QC
QSlw=0.217*QC

PB=18.6
PResp=79.1/PB
PGut=62.1/PB
PLiv=48.8/PB
PKid=79.1/PB
PRap=62.1/PB
PSlw=79.1/PB
PFat=1510.8/PB

VResp=0.0007*BW
VRespEff=VResp*PResp*PB
VRespLum=0.004667*BW
VGut=0.049*BW
VLiv=0.055*BW
VKid=0.017*BW
VRap=0.1*BW
VFat=0.07*BW
VBld=0.049*BW
VSlw=(0.8897*BW)-(VResp+VGut+VLiv+VKid+VRap+VFat+VBld)

{ Metabolic Constant Calculations }
{=====}
KMo=          88.6
lnKMC=        -5.35885
ClCo=         1.57
lnClC=        3.18103
lnKM2C=       15
lnCl2OxC=     -1.20051
KmKidLivo=    0.616
```

Perchloroethylene Inhalation Cancer Potency Values
PUBLIC REVIEW DRAFT

February, 2016

ClKidLivo= 0.0211
 VMaxLungLivo= 0.07
 VMaxTCVGo= 35.3
 lnVMaxTCVGC= 10.2
 ClTCVGo= 0.656
 lnClTCVGC= -9.17006
 VMaxKidLivTCVGo= 0.15
 ClKidLivTCVGo= 0.24

KM=KMo*exp(lnKMC)
 VMax= KM*ClCo*VLiv*exp(lnClC)

KM2=KM*exp(lnKM2C)
 VMax2=KM2*(VMax/KM)*exp(lnCl2OxC)

KMKid=KM*KMKidLivo
 VMaxKid=(VMax/KM)*KMKid*(VKid/VLiv)*ClKidLivo

KMClara=KM*PLiv/(PB*PResp)
 VMaxClara=VMax*VMaxLungLivo

VMaxTCVG=VMaxTCVGo*VLiv*exp(lnVMaxTCVGC)
 KmTCVG=VMaxTCVG/(ClTCVGo*exp(lnClTCVGC))

VMaxKidTCVG=VMaxTCVG*(VKid/VLiv)*VMaxKidLivTCVGo
 KmKidTCVG=VMaxKidTCVG/(ClKidLivTCVGo*(VKid/VLiv)*(VMaxTCVG/KMTCVG))
 {=====}

Init AGut=0 Limit AGut>=0
 Init AResp=0 Limit AResp>=0
 Init AExhResp=0 Limit AExhResp>=0
 Init AInhResp=0 Limit AInhResp>=0
 Init ALiv=0 Limit ALiv>=0
 Init AKid=0 Limit AKid>=0
 Init ARap=0 Limit ARap>=0
 Init ASlw=0 Limit ASlw>=0
 Init AFat=0 Limit AFat>=0
 Init ABld=0 Limit ABld>=0

{Respiratory Model Concentrations}
 CInhResp=AInhResp/VRespLum {conc resp lumen during inh, mg/L}
 CResp=AResp/VRespEff {conc resp tract tissue, mg/L}
 CExhResp=AExhResp/VRespLum {conc resp lumen during exh, mg/L}

{Blood Concentrations}
 CVGut=(AGut/VGut)*(1/PGut)
 CVLiv=(ALiv/VLiv)*(1/PLiv)
 CVKid=(AKid/VKid)*(1/PKid)
 CVRap=(ARap/VRap)*(1/PRap)
 CVSlw=(ASlw/VSlw)*(1/PSlw)
 CVFat=(AFat/VFat)*(1/PFat)
 CVBld=(ABld/VBld)
 CArt=(QC*CVBld+QP*CInhResp)/(QC+(QP/PB))

{Metabolism: P450 Oxidation}
 RAMetLng=(VMaxClara*CResp)/(KMClara+CResp)
 RAMetLiv1=(VMax*CVLiv)/(KM+CVLiv)+(VMax2/KM2)*CVLiv
 RAMetKid1=(VMaxKid*CVKid)/(KMKid+CVKid)

```
{Metabolism: GST Conjugation}
RAMetLiv2=(VMaxTCVG*CVLiv)/(KMTCVG+CVLiv)
RAMetKid2=(VMaxKidTCVG*CVKid)/(KMKidTCVG+CVKid)

{Respiratory Model Mass Balance Equations}
AInhResp'=QM*CIinh+DResp*(CResp-CInhResp)-QM*CIinhResp
AResp'=DResp*(CIinhResp+CEXHResp-2*CResp)-RAMetLNg
AExhResp'=QM*(CIinhResp-CEXHResp)+QP*((CArt/PB)-CIinhResp)+DResp*(CResp-CEXHResp)

{Other Mass Balance Equations}
AGut'=QGut*(CArt-CVGut)
ALiv'=(QLiv*CArt)+(QGut*CVgut)-((QLiv+QGut)*CVLiv)-RAMetLiv1-RAMetLiv2
AKid'=QKid*(CArt-CVKid)-RAMetKid1-RAMetKid2
ARap'=Qrap*(CArt-CVRap)
ASlw'=QSlw*(CArt-CVSlw)
AFat'=QFat*(CArt-CVfat)
ABld'=(QFat*CVfat)+((QGut+QLiv)*CVLiv)+(QSlw*CVSlw)+(Qrap*CVRap)+(QKid*CVKid)-
(QC*CVBld)

init MetCum=0          Limit MetCum>=0
init LivOxCum=0       Limit LivOxCum>=0

MetTot=RAMetLNg+RAMetLiv1+RAMetKid1+RAMetLiv2+RAMetKid2
MetCum'=If TIME>=336 Then (MetTot/(7*BW)) Else 0
LivOxCum'=If TIME>=336 Then (RAMetLiv1/(7*BW)) Else 0
```

{ Inhalation-Only Adaptation of Chiu and Ginsberg (2011) PCE Model
for RATS }

```
METHOD RK4
STARTTIME = 0
STOPTIME=504
DT = 0.002

ppm=50      {inhaled conc in ppm}
Cinh=If (Mod(Time,24)<=6 AND Mod(Time,168)<=120) Then (ppm*165.83/24450) Else 0

; BW=0.44   {NTP Male}
  BW=0.45   {JISA Male}
; BW=0.32   {NTP Female}
; BW=0.30   {JISA Female}

QC=13.3*BW^0.75
QP=QC*1.9*0.61643
QM=QP/0.7   {minute volume, L/h}
DResp=QP*exp(1)
; Intake=QM*Cinh*24/BW

QGut=0.153*QC
QLiv=0.021*QC
QKid=0.141*QC
QFat=0.07*QC
QRap=0.279*QC
QSlw=0.336*QC

PB=15.1
PResp=32.7/PB
PGut=40.6/PB
PLiv=50.3/PB
PKid=32.7/PB
PRap=40.4/PB
PSlw=21.6/PB
PFat=1489.3/PB

VResp=0.0005*BW
VRespEff=VResp*PResp*PB
VRespLum=0.004667*BW
VGut=0.032*BW
VLiv=0.034*BW
VKid=0.007*BW
VRap=0.088*BW
VFat=0.07*BW
VBld=0.074*BW
VSlw=(0.8995*BW)-(VResp+VGut+VLiv+VKid+VRap+VFat+VBld)

{ Metabolic Constant Calculations }
{=====}
KMo=          69.7
lnKMC=       -0.805889
ClCo=         0.36
lnClC=        2.02965
KMKidLivo=    1.53
ClKidLivo=    0.0085
VMaxLungLivo= 0.0144
```

Perchloroethylene Inhalation Cancer Potency Values
PUBLIC REVIEW DRAFT

February, 2016

VmaxTCVGo= 93.9
lnVMaxTCVGC= 10.2
ClTCVGo= 2.218
lnClTCVGC= -6.99311
VMaxKidLivTCVGo= 0.15
ClKidLivTCVGo= 0.098

KM=KMo*exp(lnKMC)
VMax=KM*ClCo*VLiv*exp(lnClC)

KMKid=KM*KMKidLivo
VMaxKid=(VMax/KM)*KMKid*(VKid/VLiv)*ClKidLivo

KMClara=KM*PLiv/(PB*PResp)
VMaxClara=VMax*VMaxLungLivo

VMaxTCVG=VMaxTCVGo*VLiv*exp(lnVMaxTCVGC)
KmTCVG=VMaxTCVG/(ClTCVGo*exp(lnClTCVGC))

VMaxKidTCVG=VMaxTCVG*(VKid/VLiv)*VMaxKidLivTCVGo
KmKidTCVG=VMaxKidTCVG/(ClKidLivTCVGo*(VKid/VLiv)*(VMaxTCVG/KMTCVG))
{=====}

Init AGut=0 Limit AGut>=0
Init AResp=0 Limit AResp>=0
Init AExhResp=0 Limit AExhResp>=0
Init AInhResp=0 Limit AInhResp>=0
Init ALiv=0 Limit ALiv>=0
Init AKid=0 Limit AKid>=0
Init ARap=0 Limit ARap>=0
Init ASlw=0 Limit ASlw>=0
Init AFat=0 Limit AFat>=0
Init ABld=0 Limit ABld>=0

{Respiratory Model Concentrations}
CInhResp=AInhResp/VRespLum {conc resp lumen during inh, mg/L}
CResp=AResp/VRespEff {conc resp tract tissue, mg/L}
CExhResp=AExhResp/VRespLum {conc resp lumen during exh, mg/L}

{Blood Concentrations}
CVGut=(AGut/VGut)*(1/PGut)
CVLiv=(ALiv/VLiv)*(1/PLiv)
CVKid=(AKid/VKid)*(1/PKid)
CVRap=(ARap/VRap)*(1/PRap)
CVSlw=(ASlw/VSlw)*(1/PSlw)
CVFat=(AFat/VFat)*(1/PFat)
CVBld=(ABld/VBld)
CArt=(QC*CVBld+QP*CInhResp)/(QC+(QP/PB))

{Metabolism: P450 Oxidation}
RAMetLiv1=(VMax*CVLiv)/(KM+CVLiv)
RAMetKid1=(VMaxKid*CVKid)/(KMKid+CVKid)
RAMetLng=(VMaxClara*CResp)/(KMClara+CResp)

{Metabolism: GST Conjugation}
RAMetLiv2=(VMaxTCVG*CVLiv)/(KMTCVG+CVLiv)
RAMetKid2=(VMaxKidTCVG*CVKid)/(KMKidTCVG+CVKid)

```
{Respiratory Model Mass Balance Equations}
AInhResp'=QM*CIInh+DResp*(CResp-CInhResp)-QM*CIInhResp
AResp'=DResp*(CIInhResp+CEXhResp-2*CResp)-RAMetLNg
AExhResp'=QM*(CIInhResp-CEXhResp)+QP*((CART/PB)-CIInhResp)+DResp*(CResp-CEXhResp)
```

```
{Other Mass Balance Equations}
AGut'=QGut*(CART-CVGut)
ALiv'=(QLiv*CART)+(QGut*CVgut)-((QLiv+QGut)*CVLiv)-RAMetLiv1-RAMetLiv2
AKid'=QKid*(CART-CVKid)-RAMetKid1-RAMetKid2
ARap'=Qrap*(CART-CVRap)
ASlw'=QSlw*(CART-CVSlw)
AFat'=QFat*(CART-CVFat)
ABld'=(QFat*CVFat)+((QGut+QLiv)*CVLiv)+(QSlw*CVSlw)+(Qrap*CVRap)+(QKid*CVKid)-
(QC*CVBld)
```

```
init MetCum=0      Limit MetCum>=0
```

```
MetTot=RAMetLNg+RAMetLiv1+RAMetKid1+RAMetLiv2+RAMetKid2
MetCum'=If TIME>=336 Then (MetTot/(7*BW)) Else 0
```

{ Inhalation-Only Adaptation of Chiu and Ginsberg (2011) PCE Model
for HUMANS }

METHOD RK4
STARTTIME=0
STOPTIME=840
DT = 0.0002

ppm=10 {inhaled conc in ppm}
CInh=ppm*165.83/24450

BW=70
QC=16*BW^0.75
QP=0.96*1.28*QC
QM=QP/0.7 {minute volume, L/h}
DResp=QP*exp(-5.06)
; Intake=QM*Cinh

QGut=0.19*QC
QLiv=0.065*QC
QKid=0.19*QC
QFat=0.05*QC
QRap=0.285*QC
QSlw=0.22*QC

PB=14.7
PResp=58.6/PB
PGut=59.9/PB
PLiv=61.1/PB
PKid=58.6/PB
PRap=59.9/PB
PSlw=70.5/PB
PFat=1450/PB

VResp=0.00018*BW
VRespEff=VResp*PResp*PB
VRespLum=0.002386*BW
VGut=0.02*BW
VLiv=0.025*BW
VKid=0.0043*BW
VRap=0.088*BW
VFat=0.199*BW
VBld=0.077*BW
VSlw=(0.8560*BW)-(VResp+VGut+VLiv+VKid+VRap+VFat+VBld)

{ Metabolic Constant Calculations }
{=====}

KMo=	55.8
lnKMC=	6.9
ClCo=	0.202
lnClC=	0.2501
KMKidLivo=	1.04
ClKidLivo=	0.0125
lnClKidLivC=	4.57452
VMaxLungLivo=	0.0128
VMaxTCVGo=	0.665
lnVMaxTCVGC=	10.2
ClTCVGo=	0.0196

Perchloroethylene Inhalation Cancer Potency Values
PUBLIC REVIEW DRAFT

February, 2016

lnClTCVGC= 5.59162
 VMaxKidLivTCVGo= 0.15
 ClKidLivTCVGo= 0.14

KM=KMo*exp(lnKMC)
 VMax=KM*ClCo*VLiv*exp(lnClC)

KMKid=KM*KMKidLivo
 VMaxKid=(VMax/KM)*KMKid*(VKid/VLiv)*ClKidLivo*exp(lnClKidLivC)

KMClara=KM*PLiv/(PB*PResp)
 VMaxClara=VMax*VMaxLungLivo

VMaxTCVG=VMaxTCVGo*VLiv*exp(lnVMaxTCVGC)
 KmTCVG=VMaxTCVG/(ClTCVGo*exp(lnClTCVGC))

VMaxKidTCVG=VMaxTCVG*(VKid/VLiv)*VMaxKidLivTCVGo
 KmKidTCVG=VMaxKidTCVG/(ClKidLivTCVGo*(VKid/VLiv)*(VMaxTCVG/KMTCVG))
 {=====}

{Metabolism: P450 Oxidation}
 RAMetLiv1=(Vmax*CVLiv)/(KM+CVLiv)
 RAMetKid1=(VMaxKid*CVKid)/(KMKid+CVKid)
 RAMetLng=(VMaxClara*CResp)/(KMClara+CResp)

{Metabolism: GST Conjugation}
 RAMetLiv2=(VMaxTCVG*CVLiv)/(KMTCVG+CVLiv)
 RAMetKid2=(VMaxKidTCVG*CVKid)/(KMKidTCVG+CVKid)

Init AGut=0 Limit AGut>=0
 Init AResp=0 Limit AResp>=0
 Init AExhResp=0 Limit AExhResp>=0
 Init AInhResp=0 Limit AInhResp>=0
 Init ALiv=0 Limit ALiv>=0
 Init AKid=0 Limit AKid>=0
 Init ARap=0 Limit ARap>=0
 Init ASlw=0 Limit ASlw>=0
 Init AFat=0 Limit AFat>=0
 Init ABld=0 Limit ABld>=0

{Respiratory Model Concentrations}
 CInhResp=AInhResp/VRespLum {conc resp lumen during inh, mg/L}
 CResp=AResp/VRespEff {conc resp tract tissue, mg/L}
 CExhResp=AExhResp/VRespLum {conc resp lumen during exh, mg/L}

{Blood Concentrations}
 CVGut=(AGut/VGut)*(1/PGut)
 CVLiv=(ALiv/VLiv)*(1/PLiv)
 CVKid=(AKid/VKid)*(1/PKid)
 CVRap=(ARap/VRap)*(1/PRap)
 CVSlw=(ASlw/VSlw)*(1/PSlw)
 CVFat=(AFat/VFat)*(1/PFat)
 CVBld=(ABld/VBld)
 CArt=(QC*CVBld+QP*CInhResp)/(QC+(QP/PB)) {arterial blood conc}

{Respiratory Model Mass Balance Equations}
 AInhResp'=QM*CInh+DResp*(CResp-CInhResp)-QM*CInhResp
 AResp'=DResp*(CInhResp+CExhResp-2*CResp)-RAMetLng
 AExhResp'=QM*(CInhResp-CExhResp)+QP*((CArt/PB)-

$$C_{InhResp} + D_{Resp} * (C_{Resp} - C_{ExhResp})$$

{Other Mass Balance Equations}

$$A_{Gut} = Q_{Gut} * (C_{Art} - C_{VGut})$$

$$A_{Liv} = (Q_{Liv} * C_{Art}) + (Q_{Gut} * C_{Vgut}) - ((Q_{Liv} + Q_{Gut}) * C_{VLiv}) - RAMetLiv1 - RAMetLiv2$$

$$A_{Kid} = Q_{Kid} * (C_{Art} - C_{VKid}) - RAMetKid1 - RAMetKid2$$

$$A_{Rap} = Q_{rap} * (C_{Art} - C_{VRap})$$

$$A_{Slw} = Q_{Slw} * (C_{Art} - C_{VSlw})$$

$$A_{Fat} = Q_{Fat} * (C_{Art} - C_{VFat})$$

$$A_{Bld} = (Q_{Fat} * C_{VFat}) + ((Q_{Gut} + Q_{Liv}) * C_{VLiv}) + (Q_{Slw} * C_{VSlw}) + (Q_{Rap} * C_{VRap}) + (Q_{Kid} * C_{VKid}) - (Q_C * C_{VBld})$$

$$MetTot = (RAMetLng + RAMetLiv1 + RAMetKid1 + RAMetLiv2 + RAMetKid2) * (24 / BW)$$

APPENDIX B

**Dose Metric Values used in Dose-Response Modeling
Obtained from PBPK Inhalation Model**

PBPK Estimated Total Metabolized Doses
(mg/kg-day)

JISA Mouse (Male and female weights: 0.048 and 0.035 kg)		
Exposure Concentration (ppm)	Male	Female
10	5.10	5.22
50	18.15	18.44
250	72.73	73.94
JISA Rat (Male and female weights: 0.45 and 0.30 kg)		
Exposure Concentration (ppm)	Male	Female
50	1.82	1.88
200	6.47	6.67
600	15.32	15.83
NTP Mouse (Male and female weights: 0.037 and 0.025 kg)		
Exposure Concentration (ppm)	Male	Female
100	32.78	33.38
200	60.25	61.40
NTP Rat (Male and female weights: 0.44 and 0.32 kg, GST Pathway metabolism for male in parenthesis)		
Exposure Concentration (ppm)	Male	Female
200	6.48	6.63
400	11.38	11.66